International Refrigeration and Air Conditioning Conference

School of Mechanical Engineering

2016

# Numerical Simulation on Forced Convection Cooling of Horizontal Ionic Wind with Multi-electrodes

Rong Li
*Key Laboratory of Refrigeration and Cryogenic Technology of Zhejiang Province / Institute of Refrigeration and Cryogenics, Zhejiang University, Hangzhou 310027, China*, 21427058@zju.edu.cn

Yijian He
yijian_he@zju.edu.cn

Guangming Chen
gmchen@zju.edu.cn

Fengshuo Wen
2470203865@qq.com

# Numerical Simulation on Forced Convection cooling of Horizontal Ionic Wind with Multi-electrodes

Rong Li[1,2], Yijian He[1,2,]*,Guangming Chen[1,2],Fengshuo Wen[1,2]

[1]Key Laboratory of the Refrigeration and Cryogenic Technology of Zhejiang Province,
Hangzhou, Zhejiang Province, China
Tel/Fax : +86 571 87952464

[2]Institute of Refrigeration and Cryogenic, Zhejiang University,
Hangzhou, Zhejiang Province, China
Tel/Fax : +86 571 87952464

* Corresponding Author
Tel/Fax : +86 571 87952464
E-mail: yijian_he@zju.edu.cn

## ABSTRACT

Enhancement of heat transfer plays an important role in the cooling of electronic or refrigeration systems, and its characteristics could strongly affect the stability and performance of such systems. To enhance heat transfer, air cooling of forced convection remains one of the main solutions. For example, conventional rotary-fan air cooling is still dominant in many areas. However, with the increasing of heat generation in these systems, the limitation of the conventional rotary-fan air cooling is become more obvious. So, demands in novel air cooling technology become necessary, e.g., silent and high efficient air cooling. Recently, ionic wind, which has no moving part and is easily miniaturized, shows great potential in heat dissipation and attracts widespread attentions. In this work, ionic wind, which is produced by wire to plate configuration for forced convection enhancement of horizontal flow along the plate, is numerically investigated. Firstly, a multi-physic model, which accounts for electric field, charge distribution, fluid dynamics, and heat transfer phenomenon, is presented. Comparisons between the simulation and literature data are conducted. Results show that better agreements are achieved by the developed model. Secondly, influences of the emitting electrodes numbers are analyzed. Results show that multiple electrodes configuration has higher performance in terms of heat transfer coefficient than that of the single electrode. Investigations are also carried out on the influences of the distances between the emitting electrodes. Thirdly, effects of the main parameters of ionic wind, such as the inlet velocity, and voltage applied on the electrodes etc., are investigated. Finally, by using the multi-physic model of ionic wind, characteristics of the heat transfer are predicted. It is found that the maximum enhancement of average heat transfer coefficient could reach around 140 %.

## 1. INTRODUCTION

Due to the rapid development of the electrical equipments, and refrigeration science and technology, an increasing heat is generated in these systems. To satisfy the need of the heat load and increase the performance of the equipments and systems, high efficient heat transfer enhancement technology is in great demand. Ionic wind has been proposed and studied as a new way to enhance heat transfer. Ionic wind is base on the corona discharge, which resulting from high electric potential difference between two electrodes with different curvatures. When the electric field density near the high curvature electrode is strong enough, the dielectric surrounds it is ionized, and the ionized particles are accelerated towards to the other electrode by the electrical force, then air flow is induced by the momentum transfer between the ionized particles and air (Fylladitakis *et al*., 2014). According to the production principle of the ionic wind, it has the advantages of no moving part and simple structures with high heat transfer rate, so it has been thought as a promising method in high efficient and silent cooling.

Ionic wind was first recorded by Hauksbee (1709), and its ability to enhance the natural convection was reported by Senftleben (1931). Since then, theoretical and experimental researches on ionic wind have been taken. The mechanism of gas movement during the corona discharge was studied by Robinson, an approximate theory related electrical and aerodynamic quantities was developed (Robinson, 1961). Stuetzer (1959) investigated the static pressure generation by ionic wind numerically and experimentally, and a theory of pressure buildup in corona discharge was present. The voltage-current characteristics of the wire to plate ionic wind was studied by Ohashi and Talaie, respectively, and the evaluated methods were proposed (Ohashi and Hidaka, 1998; Talaie *et al*., 2005).

With the development of the theory of ionic wind, the study of ionic wind applied on heat transfer enhancement attracts more attentions. In 1979, the convection heat transfer enhancement of a heated flat by ionic wind was investigated, results show that by using ionic wind, a large increase in heat transfer was obtained at low stream velocities, while at high stream velocities, this gain decreased to zero (Velkoff and Godfrey, 1979). Dulikravich *et al*. (1993) proposed a mathematical model for laminar steady flow heat transfer enhancement of ionic wind, results predicted an increase of the convective heat transfer rate was between 12 % and 64 %. Mathew *et al*. (1995) enhanced heat transfer by applying double electrodes ionic wind, visualization flow patterns, heat transfer rate and power supply were obtained, numerical results show that the maximum enhancement in heat transfer can be six times of that with no ionic wind. Thermal characteristics of laminar force convection inside a double-flow solar air heater using ionic wind was numerically investigated by Kasayapanand *et al*. (2006), it was found that the number of the electrodes can influence the enhancement of heat transfer and can also affected the solar collector efficiency. Kalman and Sher (2001) experimentally studied the performance of an electrostatic blower which creates ionic wind by a wire electrode and confined wings, the optimal parameters such as wing gap, vertical distance between electrodes etc. were found to obtain the highest velocity and heat transfer coefficient. Moreover, experimental optimize of the electrostatic blower geometry was conducted and at the optimal geometry, the heat transfer coefficient was three times higher than the free convection (Rashkovan *et al*. 2002). And in 2008, Go *et al*. (2008) experimentally investigated the external forced convection enhancement by single wire to plate ionic wind, heat transfer coefficients were obtained and a more than 200 % increase in local heat transfer was observed. Chen *et al*. (2013) applied ionic wind for enhancing LED lighting cooling, the experiment results shows 50 % decrease in thermal resistance can be obtained.

Based on the experiment data by Go *et al*. (2008), a model of forced convection cooling of horizontal ionic wind with multi-electrodes is made and simulated in present work. Current-voltage characteristics are calculated and a comparison between the simulated data and experimental data is carried out. Then, flow field of ionic wind with multi-electrodes are obtained, and the average heat transfer coefficients are calculated. Moreover, heat transfer enhancements affected by the different number of electrodes are investigated. And the optimize of the distances between the emitting electrodes are also conducted. In addition, other parameters such as the inlet velocity, and voltage applied on the electrodes etc., are changed to study their influence on the heat transfer. Finally, the cooling effectiveness of the ionic wind with multi-electrodes are discussed.

## 2. MATHMATICAL MODEL

Ionic wind is a complicated phenomenon with coupled physics of electric field, charge distribution, fluid dynamics, and thermal field. In this work, theory of electrohydrodynamic is considered to simplified the model, and a two-dimensional mathematical model is made. The governing equations for the electrical field is given

$$\nabla^2 \varphi = \frac{\rho_e}{\varepsilon} \tag{1}$$

$$\vec{E} = -\nabla \varphi \tag{2}$$

Where $\varphi$ is the electrical potential between the electrodes, and $\rho_e$ is the space charge density, $\varepsilon$ is the dielectric permittivity of air. ***E*** in equation (2) stands for the electrical field density. In order to solve these two equations the space charge distribution must be obtained. Under steady condition, the space charge is governing by the current continuity equation:

$$\nabla \cdot \vec{J} = 0 \tag{3}$$

$$\vec{J} = \mu_e \rho_e \vec{E} - D\nabla\rho_e \tag{4}$$

Where ***J*** is current density, $\mu_e$ is the ions mobility in the electric field, and *D* represents the diffusivity coefficient of ions. In equation (4), the effect of mass diffusion of the ions is considered and shown in the second term on the right side, and the first term stands for the conduction effect (Grosu and Bologa, 2008).

For flow field part of the ionic wind, a combination of Navier-Stokes equations and continuity equation for two-dimensional steady condition incompressible laminar flow is present:

$$\rho_a(\vec{u}\cdot\nabla)\vec{u} = \mu\nabla^2\vec{u} - \nabla p + \vec{F_e} \tag{5}$$

$$\nabla\cdot(\rho_a\vec{u}) = 0 \tag{6}$$

Where $\rho_a$ is the density of the fluid air, ***u*** is the velocity, $\mu$ represents the dynamic viscosity of air, *p* stands for the local pressure of the fluid, and $\boldsymbol{F_e}$ is the volume force. In the model of ionic wind, volume force is given as below (Grosu and Bologa, 2008):

$$\vec{F_e} = \rho_e\vec{E} - \frac{1}{2}\vec{E}^2\nabla\varepsilon + \frac{1}{2}\nabla[\vec{E}^2[\frac{\partial\varepsilon}{\partial\rho_a}]_T\rho_a] \tag{7}$$

The first term on the right is the electric force exerted upon free charge,  and the second term is the dielectrophoretic force, while the third term represents the electrostrictive forces within the fluid. The permittivity gradient term can be negligible in most gas, and literatures show that the electrostfiction only affect the flow in a two-phase interface (Owsenek *et al.*,1995). So the second and third term on the right hand of the equation (7) is omitted in present work, and electric force is the volume force in equation (5).

Heat transfer and temperature distribution can be obtained by the energy equation:

$$\rho_a C_p\vec{u}\cdot\nabla T = k\nabla^2 T + \mu_e\rho_e E^2 \tag{8}$$

Where *T* is the temperature of the fluid air, $C_p$ is the isobaric specific heat capacity of air, *k* is the thermal conductivity of air, *E* is the electrical field strength. The joule heating is considered and shown in the last term of the equation (8).

Based on the experiment of the Go (Go *et al.*, 2008), a rectangle simulation domain is applied and shown in Figure 1. The length and height of the rectangle domain is 125 mm and 50 mm, respectively. And the bottom boundary 2,4 and 5 of the rectangle stands for a heated flat plate. The emitter electrode 3 is placed above the flat plate, and the height of the electrodes is set as 3.15 mm, the radius of the emitter electrode is 25 um. A 6.35 mm wide collector electrode 4 is placed on the flat plate, the horizontal gap between the emitter electrode and the collector *G* is 2 mm.

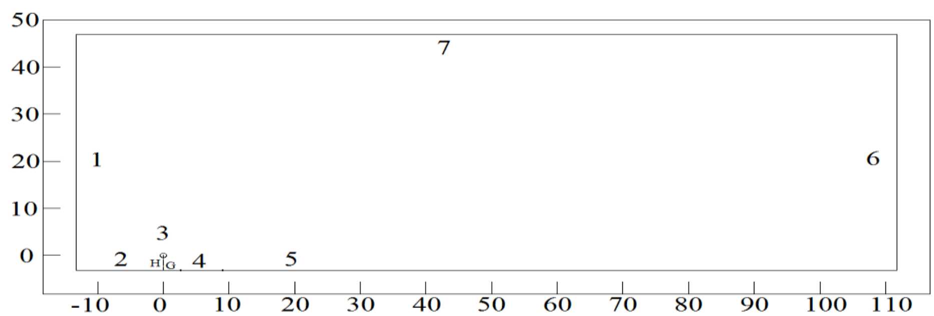

**Figure 1:** Simulation domain of the ionic wind.

To solve the equations above, appropriate boundary conditions should be given. The boundary conditions in present work are listed in Table 1.

**Table 1:** Boundary conditions for simulation

| Boundary | Electric field | Charge Transport | Fluid dynamics | Heat transfer |
|---|---|---|---|---|
| 1 | Absorbing boundary condition | Zero flux | $u=u_0$ | $T=T_{amb}$ |
| 2 | Absorbing boundary condition | Zero flux | Wall, no slip | $T=T_{plate}$ |
| 3 | $\varphi=U_0$ | $\rho_e=\rho_0$ | Wall, no slip | Adiabatic |
| 4 | $\varphi=0$ | Zero flux | Wall, no slip | $T=T_{plate}$ |
| 5 | Absorbing boundary condition | Zero flux | Wall, no slip | $T=T_{plate}$ |
| 6 | Absorbing boundary condition | Zero flux | $P_{out}=0$ | - |
| 7 | Absorbing boundary condition | Zero flux | Symmetric | - |

From Table 1, in electric field, the electric potential $U_0$ applied on the emitter electrode is given and the collector electrodes are set grounded. An initial surface charge density $\rho_0$ on the emitter electrode is obtained by the *V-I* characteristics of the ionic wind from experiment data and set as the boundary condition for charge transport equation. And the inlet velocity and temperature of the bulk flow is given. Temperature of the wall is alternated to simulate the effect of the heat load on the heat transfer.

## 3. RESULTS AND DISCUSSION

Using finite element method, the coupled equations above are solved and simulation results are obtained. The current of the single electrode model is calculated first and the comparison between the experiment data (Go *et al*., 2008) is shown in Figure 2.

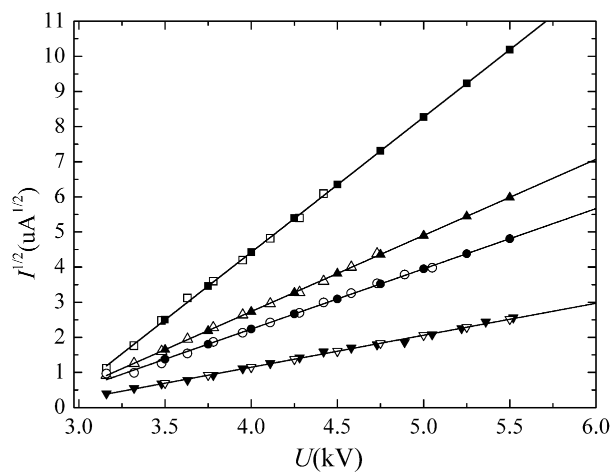


**Figure 2:** Comparison of discharge current between simulation and experiment data. □, experiment data at $G$=0 mm; ■, simulated data at $G$=0 mm; △ , experiment data at $G$=2 mm; ▲, simulated data at $G$=2 mm; ○, experiment data at $G$=4 mm;●, simulated data at $G$=4 mm;▽, experiment data at $G$=6 mm;▼, simulated data at $G$=6 mm; Solid lines are V-I characteristics of experimental data at different electrode gaps.

From the figure, the calculated currents are in good agreements with the experiment data, and the boundary conditions of the charge transport equation are verified. Then the model of force convection of horizontal ionic wind with different emitter electrodes are carried out, and simulation results are present below.

### 3.1 Force convection of horizontal ionic wind with single emitter electrode

A model of force convection of horizontal flow is established to study the heat transfer enhancement by ionic wind with single emitter electrode. The flow field are obtained and shown in Figure 3.

In Figure 3, the potential on the emitter electrode $U_0$=4.50 kV, and inlet velocity of horizontal bulk flow is 0.28 m•s$^{-1}$, the temperature on the flat plate is $T_{plate}$=343.15 K. Average heat transfer coefficient is calculated by equation (9):

$$h = \frac{Q}{A(T_{plate} - T_{amb})} \tag{9}$$

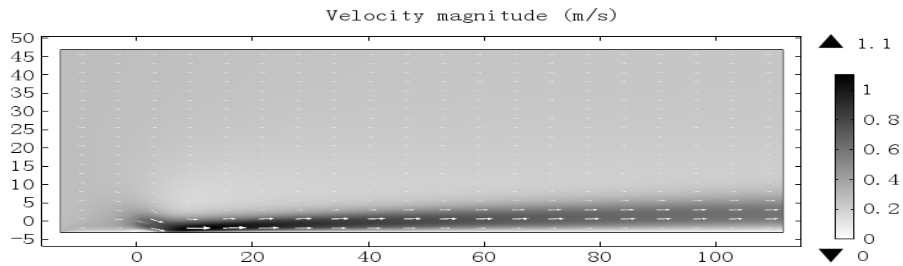


**Figure 3:** Flow field of the single electrode ionic wind

where $Q$ is the heat flux of the plate, $A$ is the area of the flat plate, $T_{amb}$ is temperature of the environment, $h$ represents the average heat transfer coefficient of the plate. Using equation (9), the average heat transfer coefficient is 33.74 W m$^{-2}$ K$^{-1}$. The maximum velocity is 1.10 m s$^{-1}$, it's almost four times that of the bulk flow, the flow accelerated strongly by the ionic wind. And from the flow pattern shown in Figure 3, the boundary layer near the plate is destroyed and rebuild, so the heat transfer is enhanced by this two effects. The percentage improvement in average heat transfer is define as (Go *et al*., 2008):

$$\Gamma = \frac{(h_{bulk+ionic} - h_{bulk})}{h_{bulk}} \times 100 \tag{10}$$

where $\Gamma$ represents the percentage improvement in average heat transfer, $h_{bulk+ionic}$ is the average heat transfer of plate with ionic wind, and $h_{bulk}$ is the average heat transfer of plate without ionic wind. Applying equation (10), a nearly 50 % improvements in average heat transfer coefficient is obtained by ionic wind with single electrode at the condition above.

The horizontal distance between the emitter electrode and the collector $G$ is varied to study its influence on heat transfer, the results are shown in Figure 4.

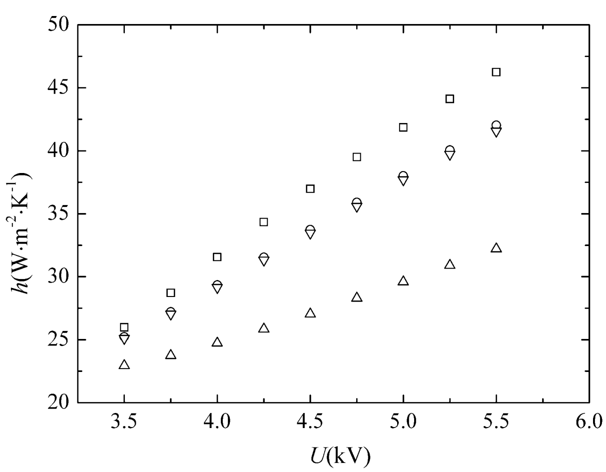


**Figure 4:** Heat transfer coefficient at different horizontal distance between the emitter electrode and the collector $G$, plate temperature is 343.15 K. □, $G$=0 mm; ○, $G$=2 mm; ▽, $G$=4 mm; △ , $G$=6 mm.

As shown in Figure 4, at the same electrical potential, with the increase of the horizontal electrode gap *G*, heat transfer coefficient decreased. Due to the small differences between the discharge currents of the *G*=2 mm and *G*=4 mm, little differences in heat transfer coefficients are observed. In addition, with the applied potential on the emitter electrode increases, the heat transfer coefficient increases, better heat transfer performance is obtained. Compared Figure 4 with the current-voltage characteristics of the ionic wind, it is found that a high discharge current lead to a high heat transfer coefficient, so the discharge current plays an important role in heat transfer enhancement of ionic wind. Choosing *G*=2 mm as default value, the other parameters of ionic wind are studied.

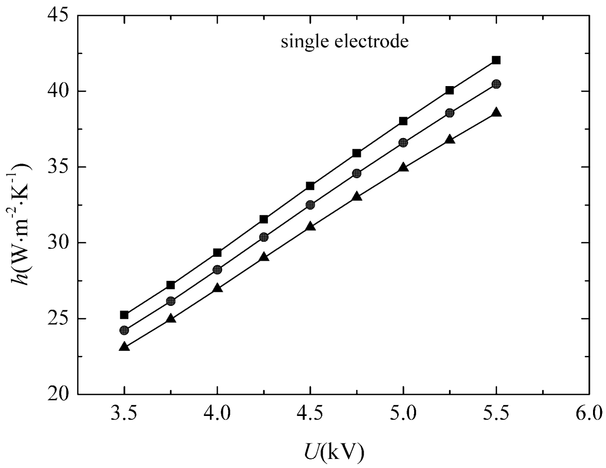


**Figure 5:** Heat transfer coefficient at different plate temperature. ■, plate temperature is 343,15 K; ●, plate temperature is 333,15 K; ▲, plate temperature is 323,15 K.

The different heating load is applied on the flat plate by setting different flat temperature. The effects of the plate temperature on the heat transfer are shown in Figure 5. In Figure 5, at the same electrical potential, the heat coefficient increases with the increase of the plate temperature, which predicted a high performance of heat transfer in high heat load area by using ionic wind.

### 3.2 Force convection of horizontal ionic wind with multi-electrodes

Since heat transfer is improved by horizontal ionic wind with single electrode, to further enhance the heat transfer, multi-electrodes structure of horizontal ionic wind is considered. In horizontal ionic wind with multi-electrodes, two or more emitter and collector electrode are applied and the simulations are carried out. In multi-electrodes model the horizontal gap between the emitter electrode and the collector *G* is 2 mm by default, temperature of the heat plate is fixed at 343.15 K. Figure 6 shows the velocity distribution of horizontal ionic wind with two and three pair of electrodes at $U_0$= 4.5 kV. Two emitter electrodes are placed at x=0, 20 mm, and the third electrode is placed at x=40 mm for three emitter electrodes condition.

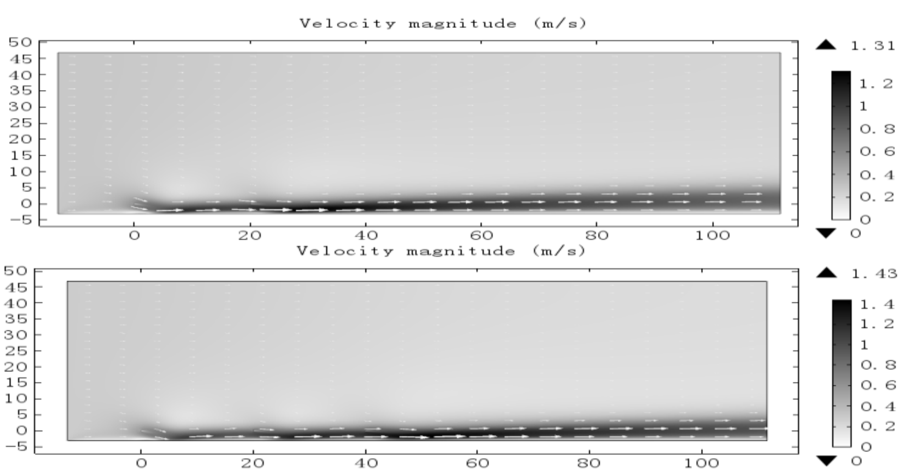


**Figure 6:** Velocity magnitude of horizon ionic wind with two or three pair of electrodes.

As shown in Figure 6, the horizontal flow are accelerated several times, and the boundary layer near the plate is disturbed repeatedly, so with the increases of the emitter electrode numbers, the maximum velocity increases, and the heat transfer can be further improved. To clearly present the performance of the heat transfer enhancement of multi-electrodes ionic wind, heat transfer coefficients are calculated and influences of the emitter electrode numbers are shown in Figure 7.

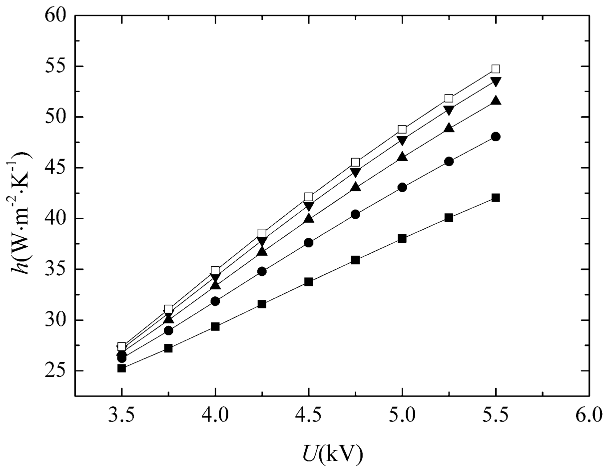


**Figure 7:** Influences of the electrode numbers on force convection of horizontal flow. ■, single emitter electrode; ●, two emitter electrodes; ▲, three emitter electrodes; ▼, four emitter electrodes; □, five emitter electrodes.

From Figure 7, five conditions of different emitter electrode numbers are investigated, and the distance between the emitter electrodes *d* are set as 20 mm, inlet velocity of horizontal bulk flow is set 0.28 m•s$^{-1}$. Results show that the increases in emitter electrode numbers lead to an increase in heat transfer coefficients. However, with the increase of emitter electrode numbers, the increases rates of heat transfer coefficients decreased. So less heat transfer enhancement per wire electrode is obtained by multiple electrodes.

Then, the optimize study of distances between the emitter electrodes *d* is carried out. Figure 8 presents the effects of the distance between the emitter electrodes *d* on heat transfer coefficients.

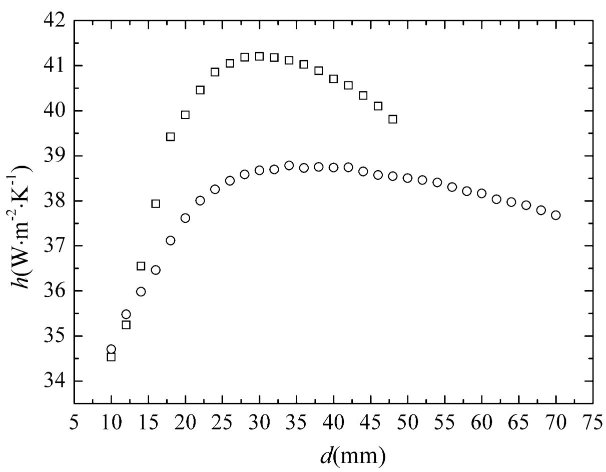


**Figure 8:** Effect of the distance between the emitter electrodes *d* on heat transfer coefficient. $T_{plate}$=343.15 K, $U_0$=4.5 kV, $u_0$=0.28 m•s$^{-1}$. □, ionic wind with two emitter electrode; ○, ionic wind with three emitter electrode.

In Figure 8, horizontal ionic wind with two and three pair of electrodes are investigated, results show that with the increase of the distance between the emitter electrodes *d*, the average heat transfer coefficient increases rapidly first, and then decreases after reaching the peak value. So there is an optimal distance between the emitter electrodes to achieve the highest heat transfer coefficient, and the optimal distance is around 30 mm at present condition.

Figure 9 shows the influence of the inlet velocity of bulk flow on the heat transfer coefficients, three pair of electrodes with 30 mm spacing are considered, the temperature of the plate is 343.15 K, and the applied potential is fixed at 4.5 kV. It is found that with the increase of the inlet velocity, the performance of heat transfer improved, but the percentage improvement in average heat transfer coefficient decreased. It means that the influence of ionic wind on bulk flow is significant at low stream velocities, when stream velocities increases, the heat transfer enhancement is dominated by the bulk flow.

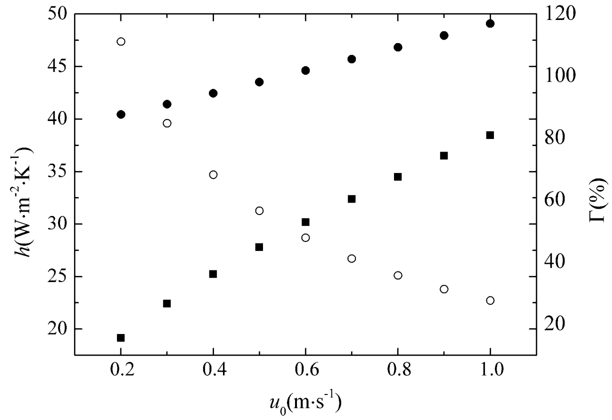


**Figure 9:** Effects of the inlet velocity of bulk flow $u_0$ on heat transfer coefficient. ■, heat transfer coefficients of bulk flow; ●, heat transfer coefficients of bulk flow with ionic wind; ○, percentage improvement in average heat transfer coefficient.

Further study on percentage improvement and cooling effectiveness is carried out. The cooling effectiveness is defined by dividing the thermal power removed by the total power input (Jewell-Larsen *et al*., 2008):

$$\eta = \frac{Q}{IU} \tag{11}$$

Where $I$ is the total current of the ionic wind, $U$ stands for the input voltage, $\eta$ is the cooling effectiveness. The cooling effectiveness shows the power consumption of the ionic wind, a high $\eta$ means the ionic wind can remove more heat at the same power input.

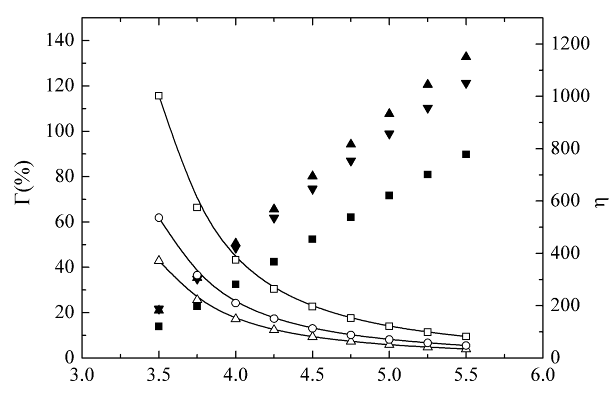


**Figure 10:** Percentage improvement in average heat transfer and cooling effectiveness of the horizontal ionic wind. ■, percentage improvement in average heat transfer of ionic wind with single electrode; ▼, percentage improvement in average heat transfer of ionic wind with two electrodes; ▲, percentage improvement in average heat transfer of ionic wind with three electrodes; □, cooling effectiveness of the horizontal ionic wind with single electrode; ○, cooling

effectiveness of the horizontal ionic wind with two electrodes; △ , cooling effectiveness of the horizontal ionic wind with three electrodes.

Both of the percentage improvements and cooling effectiveness of the horizontal ionic wind are calculated and shown in Figure 10, distance between the emitter electrodes *d* is fixed at 30 mm under multiple electrodes conditions. It is found the maximum enhancement of average heat transfer coefficient can reach 140 %, and the enhancement of average heat transfer coefficient is significant in multi-electrodes configuration. However, with the increase of the electrodes, the cooling effectiveness decreases, and though high voltage can significant improve the heat transfer, its effectiveness is low.

## 6. CONCLUSIONS

In present work, wire to plate configuration ionic wind for forced convection enhancement of horizontal flow along the plate is investigated. A two dimensional model is established and numerically simulated. Force convection of horizontal ionic wind with single electrode and multi-electrodes are studied. For single electrode, the horizontal gap *G* between the emitter and collector is changed to study its effects, the current of ionic wind and flow field are obtained, and heat transfer coefficient are calculated. Results show that heat transfer coefficient increases with the increase of the applied voltage and the decrease of the horizon gap *G*. The discharge current plays an important role in heat transfer enhancement of ionic wind, a high discharge current can brought a high heat transfer coefficient. Then the influence of the heating load of the plate is investigated, with the increase of the temperature of the flat plate, better heat transfer performance is obtained. Further study on improve the heat transfer by ionic wind with multiple electrode is present. It is found that multiple electrodes configuration predicts higher performance in terms of heat transfer coefficient than that of the single electrode. However, the increases rates of heat transfer coefficient decreased with the increase of emitter electrode numbers. The effect of the distance between the emitter electrodes are conducted, to achieve the highest heat transfer performance, an optimal spacing of around 30 mm between the emitter electrodes is obtained at present condition. Moreover, the investigation of the inlet velocities of the bulk flow shows that ionic wind plays a leading role on heat transfer enhancement at low stream velocities, with the stream velocities increases, the bulk flow would be the dominant. Finally, percentage improvement of average heat transfer coefficient and cooling effectiveness of the horizontal ionic wind are calculated. A maximum enhancement of average heat transfer coefficient around 140 % is obtained, and though the enhancement of average heat transfer coefficient is significant in multi-electrodes configuration with high applied voltage, its cooling effectiveness is relatively low. So, finding better parameters to enhance heat transfer by ionic wind at high cooling effectiveness is necessary.

## NOMENCLATURE

| | | |
|---|---|---|
| $\varphi$ | electrical potential | (V) |
| $\rho_e$ | space charge density | ($C\ m^{-3}$) |
| $\varepsilon$ | dielectric permittivity of vacuum | (–) |
| $\boldsymbol{E}$ | electrical field density vector | ($V\ m^{-1}$) |
| $\boldsymbol{J}$ | current density vector | ($A\ m^{-2}$) |
| $\mu_e$ | ions mobility coefficient | ($m^2\ V^{-1}\ s^{-1}$) |
| $D$ | diffusivity coefficient of ions | ($m^2\ s^{-1}$) |
| $\rho_a$ | density of the fluid air | ($kg\ m^{-3}$) |
| $\boldsymbol{u}$ | velocity vector of fluid | ($m\ s^{-1}$) |
| $\mu$ | dynamic viscosity of air | ($kg\ m^{-1}\ s^{-1}$) |
| $p$ | local pressure of the fluid | (Pa) |
| $\boldsymbol{F_e}$ | body force vector | (N) |
| $C_p$ | isobaric specific heat capacity of air | ($J\ kg^{-1}\ K^{-1}$) |
| $T$ | temperature of the fluid air | (Pa) |
| $U$ | applied voltage on the electrode | (V) |
| $I$ | discharge current | (A) |
| $h$ | average heat transfer coefficient | ($W\ m^{-2}\ K^{-1}$) |
| $A$ | area of the flat plate | ($m^2$) |
| $Q$ | heat power removal of the plate | (W) |
| $\Gamma$ | percentage improvement in heat transfer | (%) |

| | | |
|---|---|---|
| *d* | distance between the emitter electrodes | (mm) |
| *G* | horizon electrode gap | (mm) |
| $\eta$ | cooling effectiveness | (-) |
| x | x-coordinate | (-) |

**Subscript**

| | |
|---|---|
| e | electrical |
| a | air |
| p | pressure |
| out | out flow |
| amb | ambient |
| plate | heating flat plate |
| bulk | bulk flow |

## REFERENCES

Fylladitakis, E.D., Theodoridis, M.P. & Moronis, A.X. (2014). Review on the history, research, and applications of electrohydrodynamics. *IEEE Trans. Plasma Sci.*, *42*(42), 358-375.

Hauksbee, F. (1709). *Physico-mechanical experiments on various subjects*. London, England, 46-47.

Senftleben, H.Z. (1931). *Phys.* (32), 550.

Robinson, M. (1961). Movement of air in the electric wind of the corona discharge. *American Institute of Electrical Engineers Part I Communication & Electronics Transactions of the*, *80*(2), 143-150.

Stuetzer, O.M. (1959). Ion Drag Pressure Generation. *J. Appl. Phy.*, *30*(7). 984-994.

Ohashi, S. & Hidaka, K. (1998). A method for computing current density and electric field in electrical discharge space using current flow-line coordinate. *J. of Electrost.*, *43*(2), 101–114.

Talaie, M.R., Taheri,M. & Fathikaljahi, J. (2001). A new method to evaluate the voltage–current characteristics applicable for a single-stage electrostatic precipitator. *J. of Electrost.*, *53*(53), 221-233.

Velkoff, H.R. & Godfrey R. (1979). Low-Velocity Heat Transfer to a Flat Plate in The Presence of a Corona Discharge in Air. *J. Heat Transfer*, *101*(1), 157-163.

Dulikravich, G.S., Ahuja, V. & Lee, S. (1993). Simulation of electrohydrodynamic enhancement of laminar flow heat transfer. *J. Enhanced Heat Transfer,1*(1), 115-126.

Mathew, J. & Lai, F.C. (1995). Enhance heat transfer in a horizontal channel with double electrodes. *Industry applications Conference, 1995. Thirtieth IAS Annual meeting, IAS '95., Conference Record of the 1995 IEEE.* (1472-1479).

Kasayapanand, N., Vorayos, N. & Kiatsiriroat, T. (2006). Enhanced heat transfer in a solar air heater with double-flow configuration by electrohydrodynamic technique. *J. Enhanced Heat Transfer*, *13*(1), 39-52.

Kalman, H. & Sher, E. (2001). Enhancement of heat transfer by means of a corona wind created by a wire electrode and confined wings assembly. *Appl. Therm. Eng.*, *21*(3), 265-282.

Rashkovan, A., Sher, E. & Kalman, H. (2002). Experimental optimization of an electric blower by corona wind. *Appl. Therm. Eng.*, *22*(14), 1587-1599.

Go, D.B., Maturana, R.A., Fisher, T.S. & Garimella, S.V. (2008). Enhancement of external forced convection by ionic wind. *Int. J. Heat Mass Transfer*, *51*(25–26), 6047-6053.

Chen, I.Y., Guo, M.Z., Yang, K.S. & Wang C.C. (2013). Enhanced cooling for LED lighting using ionic wind. *Int. J. Heat Mass Transfer*, *57*(1), 285-291.

Grosu, F.P. & Bologa, M.K. (2008). Electroisothermal convection and its role in the process of heat exchange. *Surf. Eng. Appl. Elect.*, *44*(44), 187-194.

Owsenek, B.L., Seyed-Yagoobi, J, & Page, R.H. (1995). Experimental investigation of corona wind heat transfer enhancement with a heated horizontal flat plate. *J. of Heat Transfer*, *117*(2), 309-315.

Jewell-Larsen, N.E., Hsu, C.P. & Krichtafovitch, I.A. *et al*. (2008). CFD analysis of electrostatic fluid accelerators for forced convection cooling. *IEEE Trans. Dielectr. Electri. Insul.*, *15*(6), 1745-1753.

## ACKNOWLEDGEMENT

This work is supported by Cultural Heritage Bureau of Zhejiang Province (Grant No.2016008) and the National Natural Science Foundation of China (Grant No.51206140)